



HAL
open science

A Waveguide Approach for Computing Exterior Acoustic Radiation

Denis Duhamel

► **To cite this version:**

Denis Duhamel. A Waveguide Approach for Computing Exterior Acoustic Radiation. Forum Acusticum 2011, Jun 2011, Aalborg, Denmark. pp.139-144. hal-00668517

HAL Id: hal-00668517

<https://hal.science/hal-00668517>

Submitted on 9 Feb 2012

HAL is a multi-disciplinary open access archive for the deposit and dissemination of scientific research documents, whether they are published or not. The documents may come from teaching and research institutions in France or abroad, or from public or private research centers.

L'archive ouverte pluridisciplinaire **HAL**, est destinée au dépôt et à la diffusion de documents scientifiques de niveau recherche, publiés ou non, émanant des établissements d'enseignement et de recherche français ou étrangers, des laboratoires publics ou privés.

A Waveguide Approach for Computing Exterior Acoustic Radiation

Denis Duhamel

Université Paris-Est, Laboratoire Navier, ENPC/IFSTTAR/CNRS, Champs sur Marne, France

Summary

Many approaches, like the finite or boundary elements, have been used in the past for computing the radiation of wave in unbounded media. However, both methods can lead to a large number of degrees of freedom and, consequently, to heavy computations when the frequency increases. Here, a waveguide approach is proposed for solving this problem in which propagating waves are first computed on a small rib around the radiating body. The solution of the problem is then decomposed into wave components and only radiating components are kept. This allows a solution of radiation and scattering problems while limiting the discretization to a very small part of the exterior domain. Examples are given to estimate the efficiency of the proposed method.

PACS no. 43.20.Ef, 43.40.Rj

1. Introduction

Many approaches have been used in the past for computing the solutions of wave problems in unbounded media. In the domain methods a large part of the exterior domain is meshed and this computational domain is truncated at some distance where local or global boundary conditions are imposed. These conditions at finite distance must simulate as closely as possible the exact radiation condition at infinity. This approach leads to various methods like the Dirichlet to Neumann (DtN) mapping proposed by [1], the use of infinite elements proposed by [2] or the perfectly matched layer proposed by [3]. However, meshing the exterior domain leads to a large number of degrees of freedom and consequently to heavy computations when the frequency increases.

In the surface methods only the surface is meshed and this is usually done by the boundary element method described in numerous classical textbooks like [4, 5, 6]. It consists in solving an equation on the boundary of the domain only and the radiation conditions are taken into account analytically. However, the final problem usually involves full matrices which are also often non symmetrical. So this method can lead to heavy computations when the number of degrees of freedom increases, for instance for high frequencies. To try to overcome this problem, the fast multipole method was developed by [7, 8]. In this approach the

Green's function of the problem is expanded in multipole by grouping the computation of the interactions between far-away basis functions. Using a multilevel approach, the number of operations can be reduced to the order of $O(N \log N)$ where N is the number of degrees of freedom on the boundary. This considerably increases the potential of boundary element methods but this needs complicated programming and must be adapted for different Green's functions.

Here, a wave finite element method is used to find propagation constants and wave modes using finite element matrices defined on a small rib around the radiating body. This near surface condition allows an efficient solution of radiation and scattering problems by limiting the discretization to a very small part of the exterior domain. Solutions in the exterior domain are computed by using relations between layers related by homothetic transformations, so the method is named Homothetic Wave Finite Element (HWFE). The error can be controlled and the solution converges to the exact solution by using a sufficient number of layers. It is shown that the approach is more efficient for high frequencies and can be complementary of the usual methods involving traditional finite or boundary elements. This approach is based on wave finite elements which are described in [9, 10, 11, 12].

This paper is divided into four sections and is outlined as follows. In section two, waves are computed in a layer around the radiating body. In section three relations between layers are given. In section four, numerical examples are given to test the efficiency of the method before the conclusion.

2. Waves in a layer

2.1. Behaviour of a layer

Consider the general case of a convex body Ω surrounded by an infinite domain as in figure 1. Linear

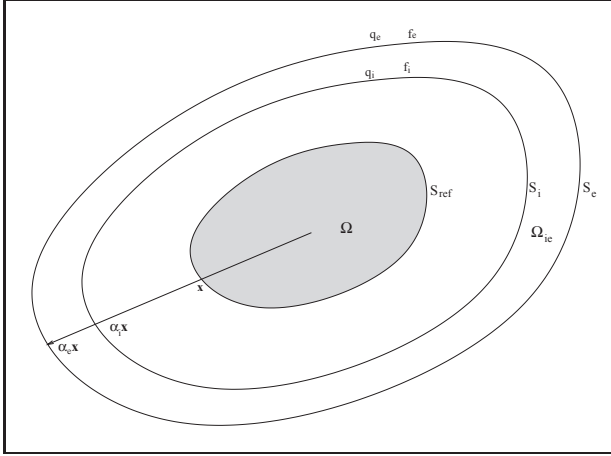


Figure 1. Exterior domain with surfaces of homothetic sizes.

waves are supposed to propagate in this exterior domain. A layer, defined as the domain Ω_{ie} between surfaces S_i and S_e , is described by a finite element model. It is supposed that the inner and outer surfaces have sizes proportional to the surfaces of the body S_0 , that means that points on these surfaces are given by $\mathbf{x}_i = \alpha_i \mathbf{x}_0$ and $\mathbf{x}_e = \alpha_e \mathbf{x}_0$ where α_i and α_e are constants on their respective surfaces. A layer can be meshed with an arbitrary number of elements using the full possibilities of usual finite element software. The discrete dynamic behaviour of a layer obtained from a finite element model at a circular frequency ω is given by

$$(\mathbf{K} - \omega^2 \mathbf{M}) \mathbf{Q} = \mathbf{F} \quad (1)$$

where \mathbf{K} and \mathbf{M} are the stiffness and mass matrices respectively, \mathbf{F} is the loading vector and \mathbf{Q} the vector of the degrees of freedom. Introducing the dynamic stiffness matrix of the layer $\mathbf{D}^L = \mathbf{K} - \omega^2 \mathbf{M}$, eliminating the interior degrees of freedom and separating the dofs into the inner (i) and outer (e) boundaries leads to

$$\begin{bmatrix} \mathbf{D}_{ii}^L & \mathbf{D}_{ie}^L \\ \mathbf{D}_{ei}^L & \mathbf{D}_{ee}^L \end{bmatrix} \begin{bmatrix} \mathbf{Q}_i \\ \mathbf{Q}_e \end{bmatrix} = \begin{bmatrix} \mathbf{F}_i \\ \mathbf{F}_e \end{bmatrix} \quad (2)$$

which describes the behaviour of the layer. By symmetry of the stiffness and mass matrices, this dynamic stiffness matrix is also symmetric.

Instead of working with the current variables defined on surfaces S_i and S_e , we will work with reference variables defined on the reference surface S_0 such

that

$$\begin{aligned} \mathbf{Q}_i &= \alpha_i^{-d} \mathbf{q}_i \\ \mathbf{Q}_e &= \alpha_e^{-d} \mathbf{q}_e \\ \mathbf{F}_i &= \frac{\alpha_i^d}{\omega} \mathbf{f}_i \\ \mathbf{F}_e &= \frac{\alpha_e^d}{\omega} \mathbf{f}_e \end{aligned} \quad (3)$$

where $d = (n - 1)/2$ and n is the space dimension. This change of variable is introduced to preserve the scalar product between functions defined on S_0 , S_i and S_e . Relation (3) should be identical in terms of displacement and force density. However, the nodal values of the force in the finite element model are obtained through an integration over surface elements and so already include a α^{2d} contribution. This leads finally to the α^d term in the relation involving the force nodal values. The $1/\omega$ term is introduced as a normalization of the scale between homothetic layers. Thus, the behaviour of a layer is now given by

$$\begin{aligned} \begin{bmatrix} \mathbf{f}_i \\ \mathbf{f}_e \end{bmatrix} &= \frac{1}{\omega} \begin{bmatrix} \alpha_i^{-2d} \mathbf{D}_{ii}^L & \alpha_i^{-d} \alpha_e^{-d} \mathbf{D}_{ie}^L \\ \alpha_i^{-d} \alpha_e^{-d} \mathbf{D}_{ei}^L & \alpha_e^{-2d} \mathbf{D}_{ee}^L \end{bmatrix} \begin{bmatrix} \mathbf{q}_i \\ \mathbf{q}_e \end{bmatrix} \\ &= \begin{bmatrix} \mathbf{D}_{ii} & \mathbf{D}_{ie} \\ \mathbf{D}_{ei} & \mathbf{D}_{ee} \end{bmatrix} \begin{bmatrix} \mathbf{q}_i \\ \mathbf{q}_e \end{bmatrix} \end{aligned} \quad (4)$$

This matrix is also symmetric.

2.2. Eigenvalue problem

In terms of the variables \mathbf{f} and \mathbf{q} , free wave propagation is described by the discrete eigenproblem

$$\begin{cases} \mathbf{q}_e = \lambda \mathbf{q}_i \\ \mathbf{f}_e + \lambda \mathbf{f}_i = 0 \end{cases} \quad (5)$$

where λ is a propagation constant between the inner and outer boundaries of the domain Ω_{ie} . Combining these two relations with relation (4) yields

$$\left(\mathbf{D}_{ii} + \mathbf{D}_{ee} + \lambda \mathbf{D}_{ie} + \frac{1}{\lambda} \mathbf{D}_{ei} \right) \mathbf{q}_i = 0 \quad (6)$$

The eigenvector \mathbf{q}_i is thus the solution of a quadratic eigenvalue problem. Taking the transpose of equation (6) shows that \mathbf{q}_i is both a right-eigenvector associated with the eigenvalue λ and a left-eigenvector associated with the eigenvalue $1/\lambda$. Since the left and right eigenproblems have identical eigenvalues, it follows that if λ is an eigenvalue then so, too, is $1/\lambda$. These represent a pair of positive- and negative-going waves.

Introducing the transfer matrix

$$\mathbf{T} = \begin{bmatrix} -\mathbf{D}_{ie}^{-1} \mathbf{D}_{ii} & \mathbf{D}_{ie}^{-1} \\ -\mathbf{D}_{ei} + \mathbf{D}_{ee} \mathbf{D}_{ie}^{-1} \mathbf{D}_{ii} & -\mathbf{D}_{ee} \mathbf{D}_{ie}^{-1} \end{bmatrix} \quad (7)$$

such that

$$\mathbf{T} \begin{bmatrix} \mathbf{q}_i \\ \mathbf{f}_i \end{bmatrix} = \begin{bmatrix} \mathbf{q}_e \\ \mathbf{f}_e \end{bmatrix} \quad (8)$$

This matrix has a right eigenvector for the eigenvalue λ_i given by

$$\Phi_i = \begin{bmatrix} \mathbf{q}(\lambda_i) \\ (\mathbf{D}_{ii} + \lambda_i \mathbf{D}_{ie}) \mathbf{q}(\lambda_i) \end{bmatrix} \quad (9)$$

and a left eigenvector associated with λ_i given by

$$\Psi_i = \left[{}^t \mathbf{q} \left(\frac{1}{\lambda_i} \right) (\mathbf{D}_{ee} + \lambda_i \mathbf{D}_{ie}) \quad {}^t \mathbf{q} \left(\frac{1}{\lambda_i} \right) \right] \quad (10)$$

where $\mathbf{q}(\lambda_i)$ and $\mathbf{q}(\frac{1}{\lambda_i})$ are the eigenvectors of (6) associated to the eigenvalues λ_i and $1/\lambda_i$ respectively. Orthogonality properties can be obtained from these relationships, so, the left and right eigenvectors are such that

$$\Psi_i \Phi_j = d_i \delta_{ij} \quad (11)$$

where d_i is some constant. A normalization of the eigenvectors could be chosen such that $d_i = 1$.

2.3. Wave decomposition in a layer

From the precedent section, it is clear that the $2N$ eigenvalues of equation (6) can be split into two sets of N eigenvalues and eigenvectors which are denoted by (λ_i, Φ_i^+) and $(1/\lambda_i, \Phi_i^-)$, with the first set such that $|\lambda_i| \leq 1$. In the case $|\lambda_i| = 1$, the first set must contain the waves propagating in the positive direction, which are such that $\text{Re} \{ (i\omega) \mathbf{q}_i^H \mathbf{f}_i \} < 0$. The inverse eigenvalue $1/\lambda_i$, in the second set, is associated with the waves such that $\text{Re} \{ (i\omega) \mathbf{q}_i^H \mathbf{f}_i \} > 0$.

These waves are now used as a basis in a layer. The inner state vector is given by the following sum of positive and negative-going waves with respective amplitudes a_i^+ and a_i^-

$$\mathbf{x}_i = \begin{bmatrix} \mathbf{q}_i \\ \mathbf{f}_i \end{bmatrix} = \sum_{i=1}^{i=N} (a_i^+ \Phi_i^+ + a_i^- \Phi_i^-) \quad (12)$$

In the same way, the outer state vector is given by

$$\mathbf{x}_e = \begin{bmatrix} \mathbf{q}_e \\ \mathbf{f}_e \end{bmatrix} = \sum_{i=1}^{i=N} \left(\lambda_i a_i^+ \Phi_i^+ + \frac{1}{\lambda_i} a_i^- \Phi_i^- \right) \quad (13)$$

3. Solution in the exterior domain

3.1. Solutions in homothetic zones

Consider now the situation of figure 2, where the body Ω is surrounded by an infinite number of layers of homothetic sizes such that the positions in zones Ω_{ii+1} and Ω_{i+1i+2} are related by $\mathbf{x}^{i+1} = \alpha \mathbf{x}^i$, where α is a constant parameter. Using the results of the precedent section, eigenvalues and eigenvectors are computed in the domain Ω_{ii+1} between surfaces S_i and S_{i+1} .

Consider the case where the discrete matrices are obtained from the discretization of a second order partial differential operator as the Laplacian in acoustics or the operator of linear elasticity for elastic wave

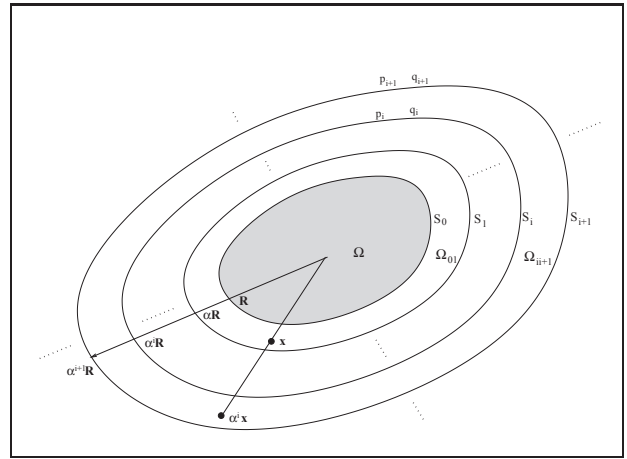


Figure 2. Exterior domain divided into zones of proportional sizes.

propagation. One gets an eigenvector in the domain Ω_{ii+1} from an eigenvector in the domain Ω_{i-1i} by

$$\begin{aligned} \Phi_j^i(\alpha \mathbf{x}, \omega) &= \Phi_j^{i-1}(\mathbf{x}, \alpha \omega) = \Phi_j^0(\mathbf{x}, \alpha^i \omega) \\ \lambda_j^i(\omega) &= \lambda_j^{i-1}(\alpha \omega) = \lambda_j^0(\alpha^i \omega) \end{aligned} \quad (14)$$

where $\Phi_j^i(\mathbf{x}, \omega)$ denotes the eigenvectors (the value of the solution on the inner surface S_i) and $\lambda_j^i(\omega)$ the eigenvalues of zone Ω_{ii+1} at the frequency ω .

Defining the state vector on the surface S_i by $\mathbf{s}^i = {}^t(\alpha^{id} \mathbf{Q}_i \quad \omega \alpha^{-id} \mathbf{F}_i)$ (with a normal towards the exterior domain), the decomposition of the solution in term of waves with amplitudes \mathbf{a}^i is given by

$$\mathbf{s}^i = \Phi^i \cdot \mathbf{a}^i = \sum_{j=1}^{j=M} a_j^i \Phi_j^i \quad (15)$$

where Φ^i is the matrix made of the Φ_j^i and \mathbf{a}^i the vector of the a_j^i .

3.2. Global solution in the exterior domain

Between two consecutive layers, one gets

$$\begin{aligned} \mathbf{s}^{i+1} &= \Phi^i \cdot \Lambda^i \cdot \mathbf{a}^i \\ &= \Phi^i \cdot \Lambda^i \cdot \Psi^i \cdot \mathbf{s}^i \\ &= \mathbf{T}^i \cdot \mathbf{s}^i \end{aligned} \quad (16)$$

where the different matrices are defined by

$$\begin{aligned} \Phi^i &= [\Phi_1^i, \dots, \Phi_M^i] \\ \Psi^i &= [\Psi_1^i, \dots, \Psi_M^i] \\ \Lambda^i &= \text{diag}[\lambda_1^i, \dots, \lambda_M^i] \\ \mathbf{T}^i &= \Phi^i \cdot \Lambda^i \cdot \Psi^i \end{aligned} \quad (17)$$

and $M = 2N$ if we retain N positive-going and N negative-going waves. So, for the complete exterior domain until surface S_n , one has

$$\begin{aligned} \mathbf{s}^n &= \mathbf{T}^{n-1} \dots \mathbf{T}^0 \mathbf{s}^0 \\ &= \mathbf{T}^0(\alpha^{n-1} \omega) \mathbf{T}^0(\alpha^{n-2} \omega) \dots \mathbf{T}^0(\omega) \mathbf{s}^0 \\ &= \mathbf{T}^{\text{tot}} \mathbf{s}^0 \end{aligned} \quad (18)$$

It is possible to compute the total matrix for different frequencies by the following recurrence relation

$$\mathbf{T}^{tot}(\omega) = \mathbf{T}^{tot}(\alpha\omega)\mathbf{T}^0(\omega) \quad (19)$$

So beginning by the highest frequency, the different total matrices can be computed by determining only $\mathbf{T}^0(\omega)$ at each frequency and by computing the product of relation (19).

Finally, the boundary condition must be such that the amplitudes of the negative going waves are null, meaning that

$$\Psi^-(\omega)\mathbf{T}^{tot}\mathbf{s}^0 = 0 \quad (20)$$

where $\Psi^-(\omega)$ is a matrix made from the left vectors Ψ_j^n associated to negative-going waves. The state vector on surface S_0 is written as

$$\mathbf{s}^0 = \begin{bmatrix} \mathbf{q}_0 \\ \mathbf{f}_0 \end{bmatrix} \quad (21)$$

and the matrix as

$$\Psi^-(\omega)\mathbf{T}^{tot} = [\mathbf{F}_0 \quad \mathbf{Q}_0] \quad (22)$$

Finally, the boundary condition can be written as the impedance condition

$$\mathbf{F}_0\mathbf{q}_0 + \mathbf{Q}_0\mathbf{f}_0 = 0 \quad (23)$$

This gives the relation on the surface of Ω approximating the radiation condition.

4. Numerical examples

We present here some examples of radiation and scattering of waves by using the precedent model. Only two-dimensional acoustic problems are computed.

4.1. Surface impedance on a cylinder

Consider the case of an annular domain meshed with one layer of four nodes linear acoustic elements. The cylinder is of radius $1m$ and the sound velocity is $c = 343m/s$. The results in figure 3 present the error between the analytical impedance and the impedance found by the present method for the case of a uniform loading (independent of the direction). Three possible thicknesses are considered for the layer and the results are plotted for different numbers of elements in the mesh. It can be seen that interesting results can be obtained with only one layer and with a limited number of degrees of freedom. The thickness $e = 0.01m$ is too large and lead to a loss of accuracy for high frequencies. So increasing the mesh density leads to much better results except when the thickness of the layer and the frequency are so large that the error is mainly controlled by the thickness.

In figure 4 the same computation is done for three thicknesses of the first layer. The matrix is computed

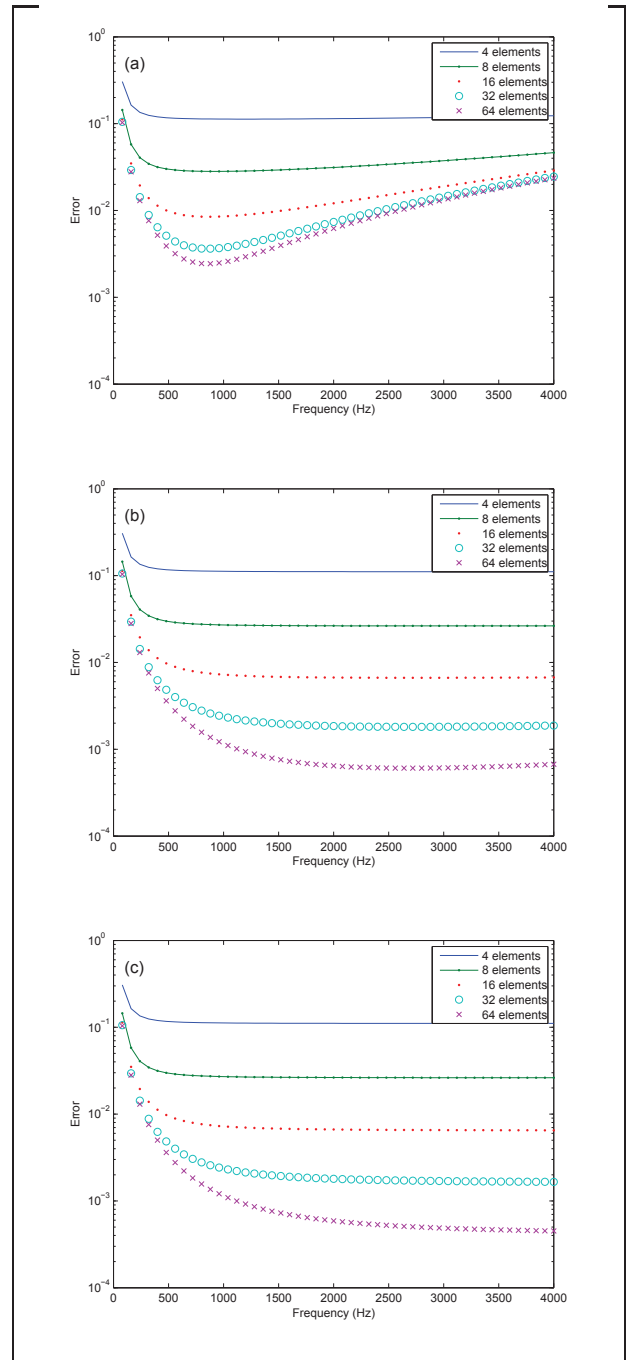


Figure 3. One layer with $e = 0.01m$ (a), with $e = 0.001m$ (b) and $e = 0.0001m$ (c).

by the recurrence relation (19) starting from the highest frequency, here $2000Hz$ and going towards lower frequencies by $f_{i+1} = f_i/\alpha$ with $f_1 = 2000Hz$. A fixed number of 200 points in frequency was used. When α is small the accuracy is better for higher frequencies but a large number of frequency points is needed to get results for low frequencies. On the contrary for large thicknesses, the frequency range is larger at the expense of a reduced accuracy.

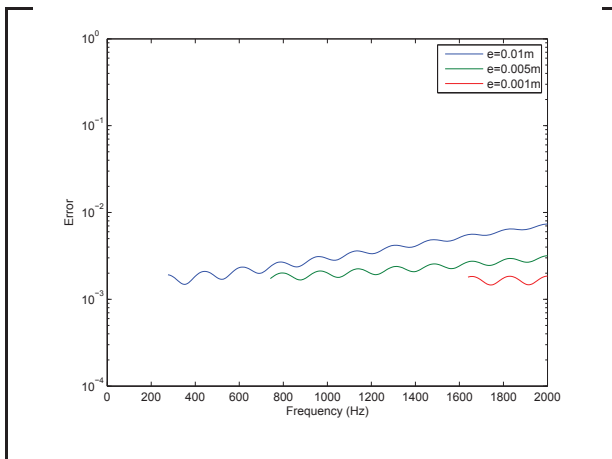


Figure 4. Error when using the recurrence relation.

4.2. Scattering by a cylinder

Consider now the problem of scattering of a point source by a rigid cylinder. The geometry is shown in figure 5. The cylinder has a radius of $1m$ and the source is located at point $(-1.5, 0)$. The mesh is made of 128 elements of thickness $0.005m$. The problem is similar to the precedent example but the force \mathbf{f}_0 of relation (23) is given by the nodal values of $-\frac{\partial p_{inc}}{\partial n}$ where p_{inc} is the incident pressure. This incident pressure is given by $\frac{i}{4}H_0(kr)$ where r is the distance between the source and the point of computation and H_0 is the Hankel function of first type and order 0. The solution of the problem allows the computation of the scattering pressure and by adding the incident pressure, the total pressure is found around the cylinder. In figure 6, the pressure around the cylinder is computed for three different frequencies. The results are presented versus the angle along the cylinder, the source being located in the direction with angle π . The pressure is computed on the surface of the cylinder and the analytical values along with the numerical results are plotted for three frequencies. It can be observed a very good agreement at low frequencies. As the frequency increases, the error also slightly increases.

4.3. Scattering by a rectangle

We study now the scattering by a rigid square of size $1m \times 1m$ as shown in figure 5. The source is located at point $(-2, 0)$ and is of unit amplitude as for the scattering by a cylinder. The surface is meshed with 64 elements and the thickness of a layer is $0.005m$. It should be noticed that the thickness is not absolutely constant as the external nodes of the layer are obtained by multiplying the distance to origin of the internal nodes by 1.005 to get a homothetic surface. The number of layers is 100. The pressure is computed version the frequency for the three points shown in figure 5. As no analytical solution is available, the results have been compared to BEM computations. The re-

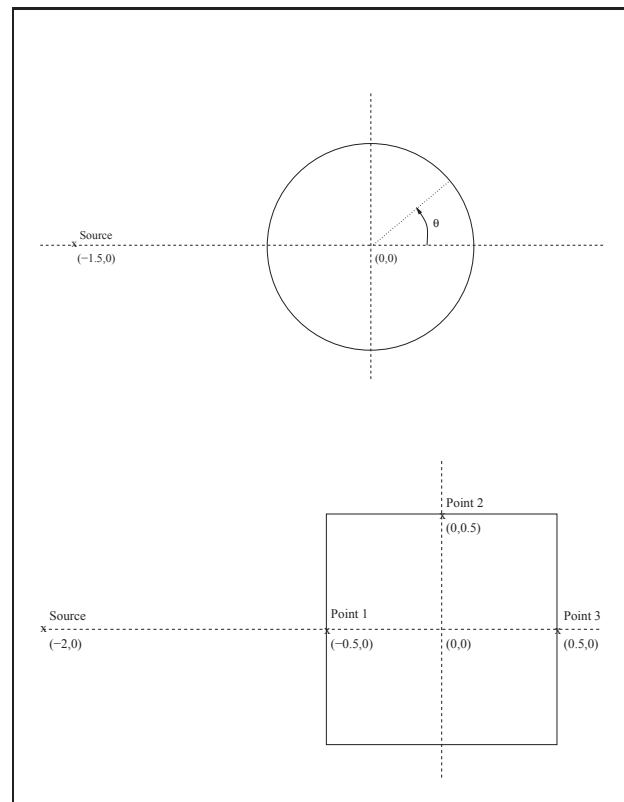


Figure 5. Geometries of the circle and the square used in the computations.

sults are presented in figure 7 and show a good agreement except for low frequencies for which the number of layers was not sufficient.

5. CONCLUSIONS

A new method founded on a waveguide approach has been proposed for the computation of radiation and scattering of waves. Homothetic relations between layers around the body allow the computation of the solution in the whole exterior domain. Examples have proved the accuracy of the method.

References

- [1] J.B. Keller, D. Givoli, A finite element method for large domains, *Comput. Methods Appl. Mech. Engrg.*, 76 (1989) 41-66.
- [2] P. Bettess, Infinite elements, *Int. J. Numer. Methods Engrg.*, 11 (1977) 53-64.
- [3] J.P. Bérenger, A perfectly matched layer for the absorption of electromagnetic waves, *J. Comput. Physics*, 114 (1994) 185-200.
- [4] C.A. Brebbia, S. Walker, *Boundary elements techniques in engineering*, Newnes-butterworths, London, England, 1980.
- [5] G. Chen, J. Zhou, *Boundary element methods, Computational mathematics and applications*, Academic press, London, 1992.

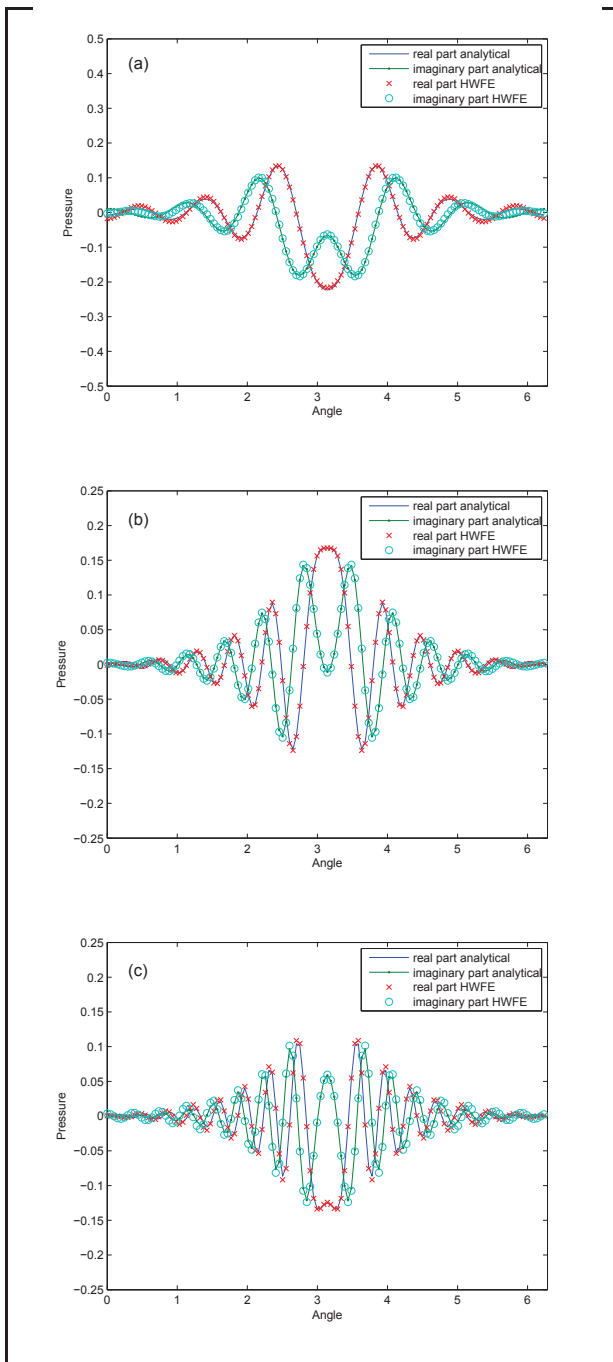


Figure 6. Pressure versus the angle along the cylinder for the frequencies 300Hz (a), 600Hz (b) and 900Hz (c) with a discretization of 128 elements.

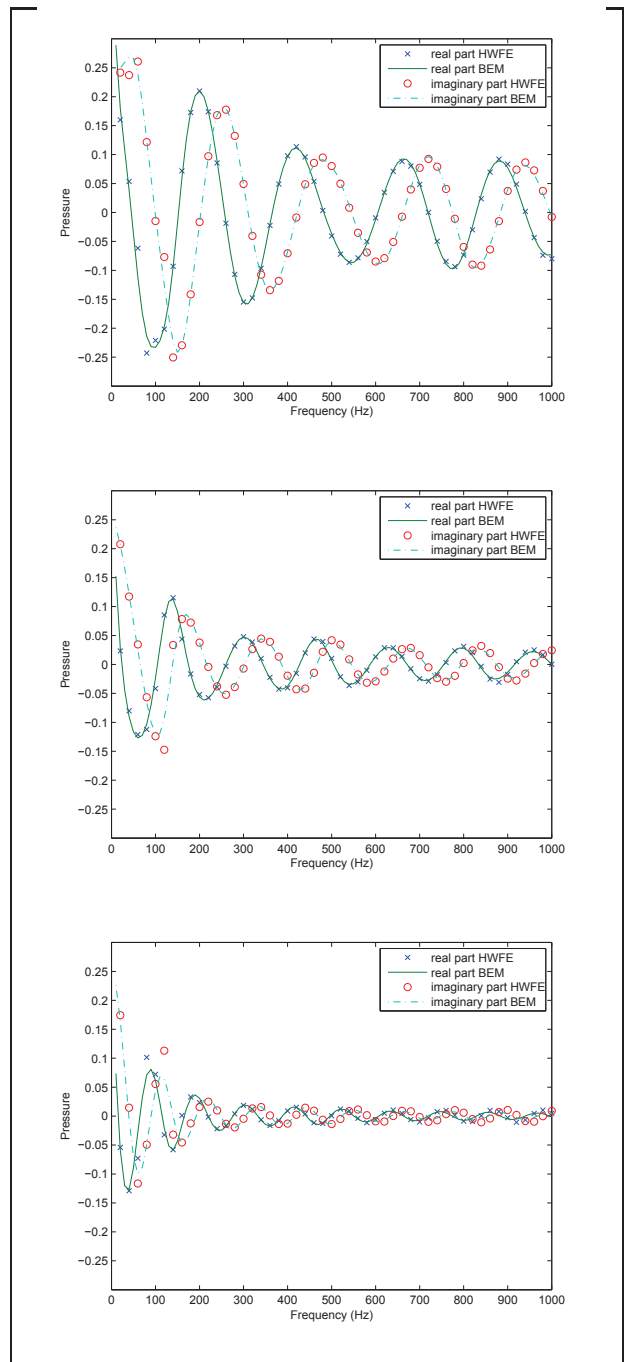


Figure 7. Pressure at three points on the surface of the square : point 1 (a), point 2 (b) and point 3 (c).

[6] M. Bonnet, Boundary integral equation methods for solids and fluids, Wiley, Chichester, England, 1995.
 [7] V. Rokhlin, Rapid solution of integral equations of classical potential theory, *J. Comput. Phys.*, 60 (1985) 187-207.
 [8] V. Rokhlin, Rapid solution of integral equations of scattering theory in two dimensions, *J. Comput. Phys.*, 86 (1990) 414-439.
 [9] D. Duhamel, T.-M. Nguyen, Finite element computation of absorbing boundary conditions for time-harmonic wave problems, *Comput. Meth. Appl. Mech. and Eng.*, 198 (2009) 3006-3019.

[10] B.R. Mace, D. Duhamel, M.J. Brennan, L. Hinke, Finite element prediction of wave motion in structural waveguides, *J. Acous. Soc. Amer.*, 117 (2005) 2835-2843.
 [11] D. Duhamel, B.R. Mace, M.J. Brennan, Finite element analysis of the vibrations of waveguides and periodic structures, *J. Sound Vib.*, 294 (2006) 205-220.
 [12] D. Duhamel, Finite element computation of Green's functions, *Engrg. Anal. Bound. Elem.*, 31 (2007) 919-930.